European Journal of Nuclear Medicine and Molecular Imaging (2019) 46:2289–2297
https://doi.org/10.1007/s00259-019-04438-w

ORIGINAL ARTICLE

Comparison of PSMA-ligand PET/CT and multiparametric MRI for the detection of recurrent prostate cancer in the pelvis

Ali Afshar-Oromieh[1,2] · Bernd Vollnberg[1] · Ian Alberts[1] · Alexandrine Bähler[3] · Christos Sachpekidis[1] · Lotte Dijkstra[1] · Fabian Haupt[3] · Silvan Boxler[4] · Tobias Gross[4] · Tim Holland-Letz[5] · George Thalmann[4] · Johannes Heverhagen[3] · Axel Rominger[1] · Kirsi Härmä[3] · Martin H. Maurer[3]

Received: 15 May 2019 / Accepted: 11 July 2019 / Published online: 27 July 2019

Abstract

Purpose So far, there have been very few studies which provide a direct comparison between MRI and PSMA-ligand PET/CT for the detection of recurrent prostate cancer (rPC). This present study therefore aims to provide further clinical data in order to resolve this urgent clinical question, and thereby strengthen clinical recommendations.

Methods A retrospective analysis was performed for patients who were scanned at our institution with whole-body PSMA-PET/CT (tracer: 68Ga-PSMA-11) between January 2017 and September 2018 in order to detect rPC. Amongst them, 43 underwent an additional pelvic MRI within 2 months. Both modalities were compared as follows: a consensus read of the PET data was performed by two nuclear physicians. All lesions were recorded with respect to their type and localization. The same process was conducted by two radiologists for pelvic MRI. Thereafter, both modalities were directly compared for every patient and lesion.

Results Overall, 30/43 patients (69.8%) presented with a pathologic MRI and 38/43 (88.4%) with a pathologic PSMA-PET/CT of the pelvis. MRI detected 53 pelvic rPC lesions (13 of them classified as "uncertain") and PSMA-PET/CT detected 75 pelvic lesions (three classified as "uncertain"). The superiority of PSMA-PET/CT was statistically significant only if uncertain lesions were classified as false-positive.

Conclusions PSMA-PET/CT detected more pelvic lesions characteristic for rPC when compared to MRI. In order to detect rPC, a potential future scenario could be conducting first a PSMA-PET/CT. Combining the advantages of both modalities in hybrid PET/MRI scanners would be an ideal future scenario.

Keywords Prostate cancer · PET/CT · PSMA · Prostate-Specific Membrane Antigen · 68Ga-PSMA-11 · MRI

This article is part of the Topical Collection on Oncology – Genitourinary

Ali Afshar-Oromieh, Bernd Vollnberg, Kirsi Härmä, Martin H. Maurer and contributed equally to the work.

✉ Ali Afshar-Oromieh
ali.afshar@insel.ch

[1] Department of Nuclear Medicine, Inselspital, Bern University Hospital, University of Bern, Bern, Switzerland

[2] Department of Nuclear Medicine, INF 400, 69120 Heidelberg, Germany

[3] Department of Radiology, Inselspital, Bern University Hospital, University of Bern, Bern, Switzerland

[4] Department of Urology, Inselspital, Bern University Hospital, University of Bern, Bern, Switzerland

[5] Department of Biostatistics, German Cancer Research Center, Heidelberg, Germany

Introduction

Prostate cancer (PC) is the most frequently diagnosed malignant tumor in men, with increasing incidence worldwide [1, 2]. Despite initial therapy, biochemical recurrence is observed in up to 40% of patients within 10 years [3, 4]. Accurate staging in such patients is challenging for conventional imaging modalities, and it is in this setting that combined positron emission and computed tomography (PET/CT) imaging using 68Ga-PSMA-11 targeting the prostate-specific membrane antigen (PSMA) [5–11] has gained rapid acceptance. PSMA is a transmembrane protein, which is strongly over-expressed in the majority of prostatic adenocarcinomas, thereby providing an ideal target for molecular imaging as well as therapy in what has come to be termed a theranostic approach [12–14].

Likewise, multi-parametric imaging (mpMRI) of the prostate is a readily available and well-established technique for

Table 1 Characteristics of patients included in this study. Time window between PET and MRI: on average, the PET was conducted 9.6 days earlier than the MRI (hence the minus signs for mean, range, and median in that row). Overall, 18 MRI were conducted before the PET and 25 PET were conducted before the MRI

Parameter	Values
Age (years): mean/standard deviation/range/median	69.8/6.2/59–86/70
GSC (mean/standard deviation/range/median)	7.5/0.9/6–9/7
PSA (ng/ml): mean/standard deviation/range/median	4.1/5.1/0.2–20/1.9
Time PET Δ MRI (days): mean/standard deviation/range/median	−9.6/33.7/−52–60/−17
Initial therapy	RP ($n = 34$)
	RP + adjuvant RT ($n = 7$)
	RT ($n = 2$)
Initial TNM	T2 ($n = 16$)
	T3 (n = 32)
	N0 ($n = 30$)
	N1 ($n = 11$)
	Nx ($n = 1$)
Injected activity (MBq): mean/standard deviation/range/median	194.6/22.3/137–235/200

RT: radiation therapy of the prostate or prostate fossa. GSC: Gleason score. [d]: days. RP: radical prostatectomy

the evaluation of prostate cancer, offering excellent spatial resolution and clear delineation of anatomical structures, including marginal invasion of surrounding structures such as the rectum, which are less easily discerned in PET/CT.

Meanwhile, 68Ga-PSMA-11 PET/CT has become a well-established methodology for imaging recurring prostate cancer (rPC), with high reported sensitivity and specificity [5, 10, 15–19]. So far, there have been very few published studies which provide a direct comparison between MRI and PSMA-ligand PET/CT for the detection of rPC. As a consequence, until recently there were no guidelines as to which modality is preferred. The most recent guidance from the European Association of Urology provides only weak evidence for the use of PSMA-ligand PET/CT in the setting of biochemical recurrence post radical prostatectomy, and unclear guidance as to which modality is preferable in the setting of recurrence post radiotherapy. This present study therefore aims to provide further clinical data in order to resolve this urgent clinical question, and thereby strengthen clinical recommendations.

Material and methods

Patients and inclusion criteria

We conducted a retrospective analysis of all patients consecutively referred to our clinic for the investigation of biochemically recurrent PC (rPC), and who were scanned with 68Ga-PSMA-11 PET/CT at our department between January 2017 (first introduction of this modality at our institute) and September 2018 ($n = 324$). Of these, 43 patients (13.3%) also underwent a MRI scan of the pelvis within a time interval of 60 days, allowing for a direct intra-patient comparison of the two modalities with particular reference to the detection of rPC in the pelvis. Patient characteristics are shown in Table 1.

Radiotracer for PET/CT imaging

68Ga-PSMA-11 was produced as previously described [5, 20]. Briefly, 68Ga3+ was obtained from a 68Ge/68Ga radionuclide generator and used for radiolabelling of PSMA-11. The 68Ga-PSMA-11 solution was applied to the patients via an intravenous bolus injection (mean of 194.6 ± 22.3 MBq, range 137–235 MBq). The targeted dose was 3 MBq per kilogram.

PET/CT imaging

The patients of the study population were investigated with two BIOGRAPH-mCT PET/CT scanners (Siemens, Erlangen, Germany) which were cross-calibrated.

In 2017, the patients (19 of them included in this study) were scanned at 1 h post injection. In 2018, the patients (24 of them included in this study) were scanned 1.5 h after tracer injection and 20 mg of furosemide (0.5 h before the scan). First, a non-contrast-enhanced CT scan from pelvis to vertex was performed using the following parameters: slice thickness of 5 mm; increment of 3.0 mm; soft-tissue reconstruction kernel; maximum of 120 keV and 90 mAs by applying CARE kV and CARE Dose. Immediately after CT scanning, a whole-body PET (pelvis to vertex) was acquired in 3D (matrix: 200 × 200) with a zoom factor of 1. For each bed position (16.2 cm, overlapping scale: 4.2 cm), a 2 min acquisition time with a 15.5 cm field of view (FOV) was used. The emission data were corrected for randoms, scatter, and decay. Reconstruction was conducted with an ordered subset expectation maximization algorithm (OSEM) with four iterations/21 subsets and Gauss-filtered to a transaxial resolution of

5 mm at full width at half maximum (FWHM). Attenuation correction was performed using the low-dose non-enhanced computed tomography data. PET and CT were performed using the same protocol for every patient.

PET/CT analysis

PET/CT analysis was performed using an appropriate workstation and software (SyngoVia; Siemens, Erlangen, Germany). A consensus read of the scans was performed by two nuclear medicine physicians with 14 and 7 years of clinical experience (co-first authors) who were not aware of the MRI results. All lesions that were visually considered as suggestive for PC were recorded with respect to their type (local recurrence, lymph node, bones), their diagnostic certainty (0 = no tumor; 1 = clear rPC; 2 = uncertain/equivocal lesion) and location including the differentiation between inside or outside the pelvis. In a second round, both modalities (PET/CT and MRI) were directly compared for every patient and lesion by the second first author and the last author in order to note all matches and discrepancies. During this latter analysis, care was taken that the PET-findings were within the field of view of the MRI. PET-positive lesions outside the field of view of the MRI were noted separately.

MR imaging

For patients undergoing MR imaging in our clinic, a 3 Tesla (T) MR scanner (Siemens Skyra, Siemens Healthineers, Erlangen, Germany) with a specific imaging protocol for the prostate was used. The protocol consisted of an initial T2-weighted (T2w) single slab 3D TSE sequence with slab selective, variable excitation pulse [T2 SPACE, 1 mm slice thickness (ST)] which was reconstructed in an additional coronal and sagittal plane, followed by a further T2w sequence with a focus to the prostatic fossa (3 mm ST). Two separately performed sequences with diffusion-weighted imaging (DWI; b-values 0, 500, 1000, 2000) and apparent diffusion coefficient (ADC) were both focused on the whole pelvis and again the prostatic fossa. T1-weighted (T1w) axial VIBE sequences (2 mm ST) were included before and after contrast medium administration. During contrast injection, T1w VIBE perfusion imaging was performed.

MRI analysis

All MR examinations were analyzed in a consensus read by two radiologists (co-last authors) with at least 5 years' experience in MR imaging of the prostate and who were not aware of the PET/CT results. In a first round, it was assessed whether MR imaging revealed a recurrent lesion in the prostatic fossa or otherwise in the pelvis. If a recurrent lesion was detected, both its exact location and the diagnostic certainty of its presence were documented (0 = no recurring tumor; 1 = clear rPC; 2 = uncertain/equivocal finding for rPC).

Of the 43 patients included, 37 patients underwent MR imaging within our institute. Six patients underwent MR imaging at external practices. The imaging protocols of these examinations were similar, although perfusion imaging after contrast injection was missing in three cases.

Statistical analysis

Comparison of the two imaging modalities was performed by means of a two-sided McNemar test. A p value of < 0.05 was considered statistically significant.

Follow-ups

Information regarding clinical follow-up was available for 42 patients at the time of submission of this manuscript.

Results

Number of lesions detected by PET/CT versus MRI.

As presented by Table 2, MRI detected 53 PC lesions, of which 42 were classified as certain (class 1 diagnostic certainty) and 13 as "uncertain" (class 2 diagnostic certainty).

As also shown by Table 2, PSMA-PET/CT detected 75 pelvic lesions (in the same field of view as the MRI) of which three were classified as "uncertain" (class 2 diagnostic certainty). In the corresponding MRI, one of the three beforementioned lesions was classified as certain local recurrence while two lymph nodes were classified as not pathologic.

Intra-patient analysis

For each patient ($n = 43$), we then considered which imaging modality was positive and which negative. Counting the uncertain lesions (class 2 diagnostic certainty) as false-positive

Table 2 Number of lesions classified as "certain" or "uncertain" in both MRI and PSMA-ligand PET/CT

Number of certain PC lesions	MRI_{pelvin}	PET_{pelvin}
Local relapse	24	31
Lymph node met.	12	32
Bone met.	4	9
Total	40	72
Number of uncertain PC lesions	MRI_{pelvin}	PET_{pelvin}
Local relapse	5	1
Lymph node met.	6	2
Bone met.	2	0
Total	13	3

met. = metastases

(no tumor), we noted that for patients with negative (non-pathologic) MRI ($n = 14$), five patients had a negative PET and nine had a positive (pathologic) PET. Conversely, for patients with a positive MRI ($n = 29$), two had a negative PET and 27 had a positive PET. Using the McNemar test, PSMA-PET/CT was significantly ($p = 0.035$) more often pathologic compared to MRI when uncertain lesions were counted as negative.

We then repeated the analysis, this time counting the uncertain lesions (class 2 diagnostic certainty) as true-positive (tumor). In this case, for patients with a negative MRI ($n = 8$), three had a negative PET and five had a positive PET. For patients with a positive MRI ($n = 35$), two had a negative PET and 33 had a positive PET. In this case, PSMA-PET/CT was not significantly ($p = 0.257$) more often pathologic compared to MRI.

In Figs. 1, 2, 3, 4, and 5, we present examples of matched or discrepant findings of both modalities.

Detection of metastatic lesions

PSMA-PET/CT detected extrapelvic lesions (therefore outside the field of view of the MRI) in 12 different patients. Amongst them were six retroperitoneal lymph node metastases in four patients, six bone metastases in six different patients, disseminated bone metastases in one patient, and one lung metastasis in one patient.

Sequencing of the examinations

Eighteen MRI were conducted before the PET, and 25 PET were conducted before the MRI. All further details regarding the time window between the two modalities are presented in Table 1.

Follow-up

Clinical follow-up was available for 42 patients at the time of writing of this manuscript. Details regarding the different therapeutic modalities after the scans, including subsequent PSA changes, are presented by Fig. 6. None of the patients had surgical treatment or biopsies after the scans.

Of the 21 patients with a pathologic scan who were treated exclusively by radiation therapy, 14 had clearly pathologic findings in both MRI and PET, four had a clearly pathologic PET scan but an uncertain MRI scan, one had a clearly pathologic MRI but an uncertain PET scan, and two had a negative MRI but a clearly pathologic PET scan.

Summarizing the above-mentioned results, all PSMA-positive lesions and lesions suspicious of rPC in the MRI which were further treated with RT were most likely true-positive due to the subsequent decrease of PSA. Calculating the patient-based specificity, and negative and positive predictive values, was not possible because

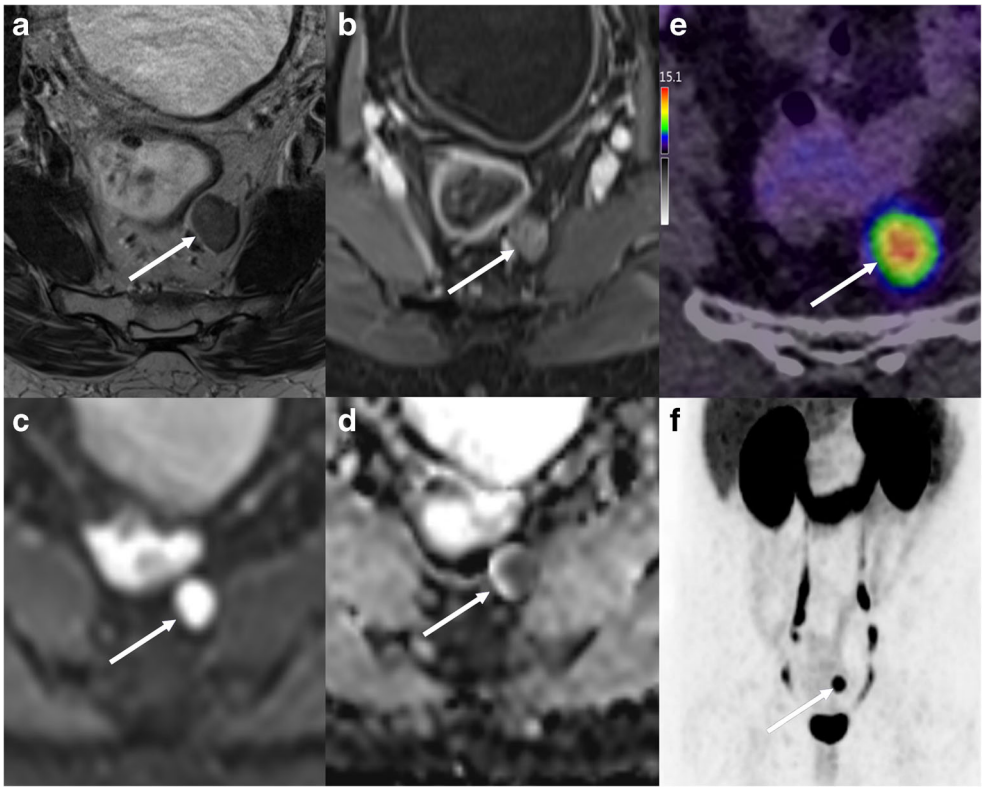

Fig. 1 A 70-year-old patient after prostatectomy with a recent minor increase of his prostate specific antigen(PSA) level to 2.6 ng/ml. An MRI of the pelvis reveals an enlarged contrast enhancing perirectal lymph nodewith a diameter of 12 mm (**a** and **b**). As there is a diffusion restriction to be detected within the lymph node (**c**,diffusion weighted imaging (DWI), b1000 image, *arrow*; **d**, apparent diffusion coefficient (ADC) map, *arrow*) a lymph node metastasis is highly likely. As the 68GaPSMA 11 PET/CT shows a strong tracer uptake (**e** and **f**-,*arrow*), there also is an urgent suspicion of a lymph node metastasis. **a**–**d**: MRI; **e**–**f**: 68Ga PSMA 11 PET/CT;**a**: T2w; **b**: contrast-enhanced T1w; **c**: b1000 DWI; **d**: ADC map; **e**: fusion of 68Ga PSMA 11 PET and low-dose CT; **f**: maximum intensity projection of the PET

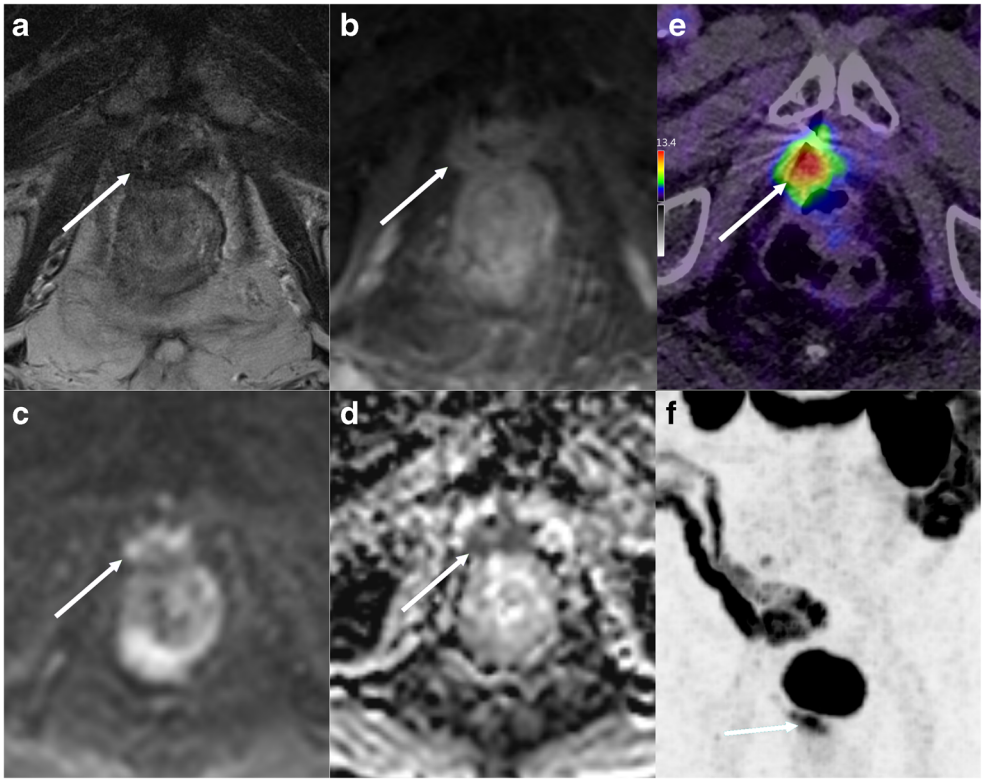

Fig. 2 Example of a consistent evaluation using MRI and 68Ga PSMA 11 PET/CT. In a follow-up examinationafter prostatectomy, a 87-year-old patient had an increase of the PSA level up to 13 ng/ml. There is a 19-mmtumorous lesion in the anterior prostate fossa in the pelvic MRI scan (**a**, T2w, *arrow*; and **b**, contrast-enhancedT1w sequence, *arrow*). A diffusion restriction (**c**, b1000, *arrow*; and **d**, corresponding ADC map, *arrow*) makethe presence of a large recurring prostate cancer very likely. In the same way, also in the 68Ga PSMA 11PET/CT there is a tumor recurrence with strong tracer uptake highly likely to be diagnosed (*arrow* in **e** and **f**).**a**–**d**: MRI; **e**–**f**: 68Ga PSMA 11 PET/CT;**a**: T2w; **b**: contrast-enhanced T1w; **c**: b1000 DWI; **d**: ADC map; **e**: fusion of 68Ga PSMA 11 PET and low-dose CT; **f**: maximum intensity projection of the PET

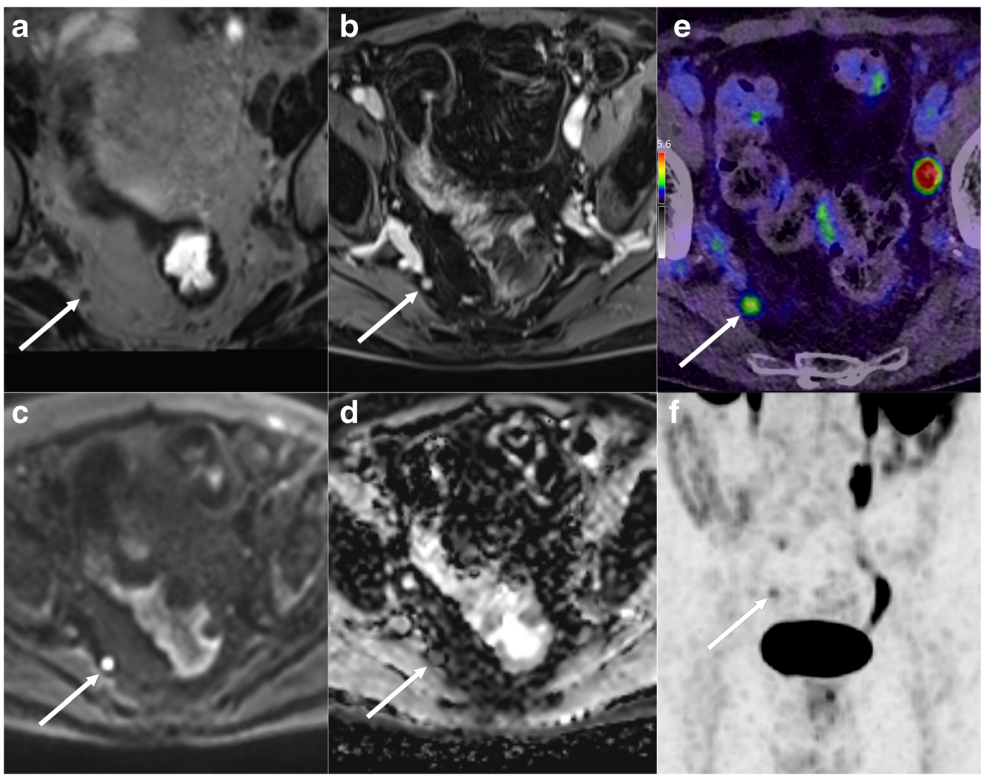

Fig. 3 Example of a small round-shaped lymph node in the right perirectal space (**a** and **b**, *arrows*). Despite thesmall size with a diameter of only 3 mm, the diffusion restriction (**c**, b1000, *arrow*; and **d**, ADC map, *arrow*)indicates a metastastic involvement. This is consistent with the increased tracer uptake in the 68Ga PSMA 11PET/CT. **a**–**d**: MRI; **e**–**f**: 68Ga PSMA 11 PET/CT;**a**: T2w; **b**: contrast-enhanced T1w; **c**: b1000 DWI; **d**: ADC map; **e**: fusion of 68Ga PSMA 11 PET and low-dose CT; **f**: maximum intensity projection of the PET

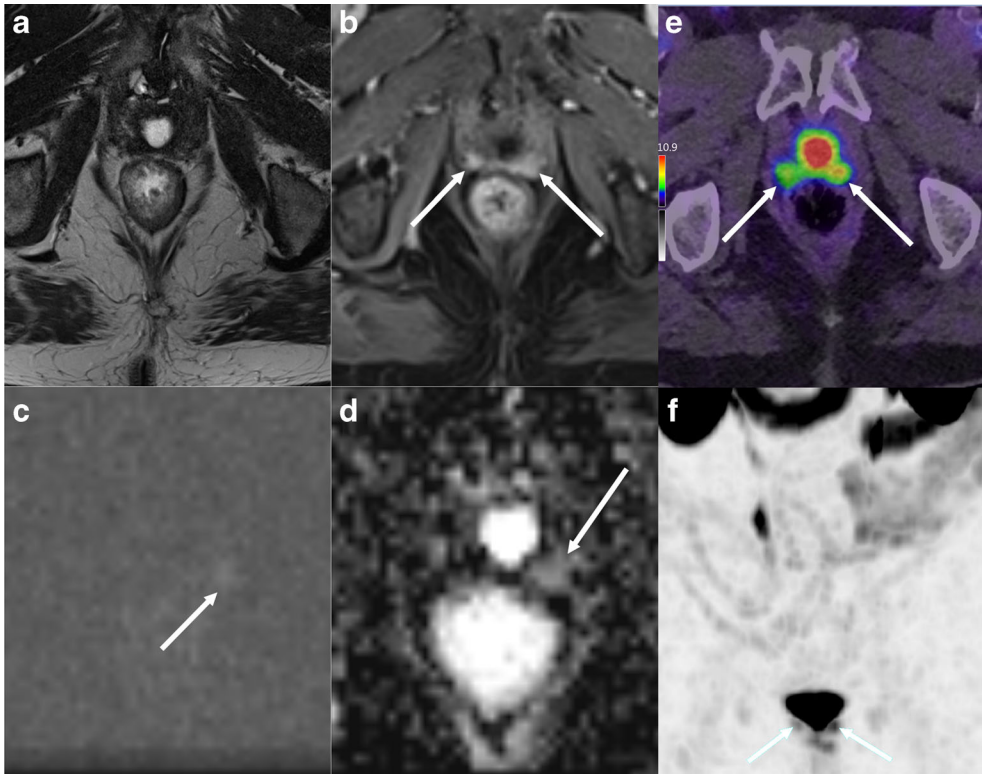

Fig. 4 Mismatch in the evaluation of a possible tumor recurrence in the prostatic fossa. After prostatectomy, inthe MRI of a 70-year-old patient an increased contrast enhancement was observed on both sides in the prostaticfossa in the contrast dynamic (DCE, dynamic contrast enhancement), especially on the left side (**b**, *right arrow*),but much less on the right side (**b**, *left arrow*). In diffusion-weighted imaging, a diffusion restriction isrecognizable only on the left side (**c** and **d**, *arrow*), but not on the right side (**c** and **d**, *dotted circle*). In contrastto this, there is an urgent suspicion of the presence of tumor recurrences on both sides in the 68Ga PSMA 11PET/CT (**e** and **f**, *arrows*). **a**–**d**: MRI; **e**–**f**: 68Ga PSMA 11 PET/CT;**a**: T2w; **b**: contrast-enhanced T1w; **c**: b1000 DWI; **d**: ADC map; **e**: fusion of 68Ga PSMA 11 PET and low-dose CT; **f**: maximum intensity projection of the PET

our cohort did not include true-negative patients (all presented with a biochemical failure).

Discussion

MRI and PET/CT imaging with PSMA ligands are both well-established and widely used imaging modalities for the investigation of prostate cancer. In the setting of rPC, both modalities having distinct advantages and disadvantages. The accurate staging of rPC is of paramount importance and guides clinical decision-making in the choice between local treatment with curative intent, systemic therapy in metastatic disease or palliative management. Furthermore, new treatment paradigms such as PSMA-ligand endoradiotherapy, or image-guided radiotherapy [21] place further demands on imaging modalities, particularly in the detection of rPC at early stages when the chance of curative treatment is at its highest. One potential solution to this conundrum is to combine the advantages of PET with MRI. Indeed, previous studies have demonstrated the advantages of this approach [22]. However, although highly promising, until hybrid PET/MRI scanners become more widely available, the question of which modality should be performed and when remains urgent.

With this in mind, there is a paucity of head-to-head comparisons between PSMA-ligand PET/CT and MRI for the detection of rPC in the literature, with truly objective comparison impeded by the heterogeneity of protocols, tracers, and patient populations. The here-presented study aimed to provide further clinical data in order to strengthen clinical recommendations.

Our retrospective study of patients referred for both imaging modalities ($n = 43$) demonstrated that 68Ga-PSMA-11 PET/CT revealed pelvic lesions characteristic of rPC in 38 patients (88%), whereas MRI revealed lesions characteristic of rPC in 30 patients (69%). Therefore, MRI-based imaging alone would have incorrectly under-staged 8/43 patients (19%) of our cohort.

Interestingly, our statistical analysis revealed that 68Ga-PSMA-11 PET/CT outperforms MRI when the equivocal results were disregarded. Only when equivocal results were included in the analysis did the two modalities reach equivalence (i.e., no statistically significant difference between the two). The reason for this lies in the finding that the number of uncertain lesions in the MRI was four times higher compared to PET/

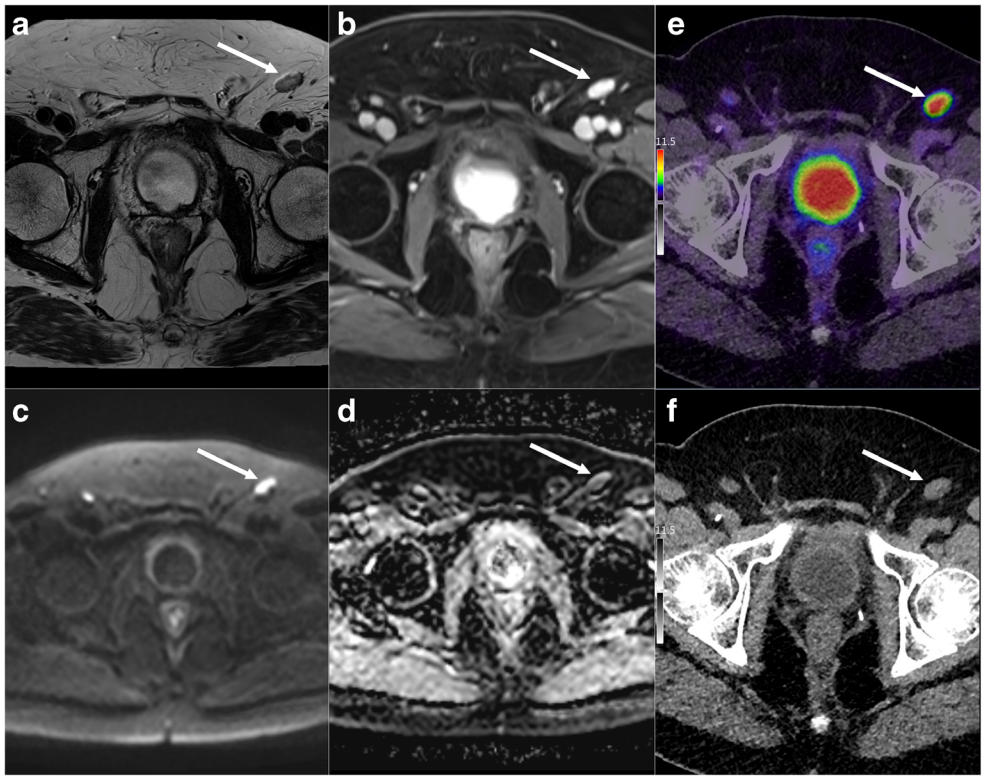

Fig. 5 Mismatch in the evaluation of a possible tumor recurrence in an iliac lymph node. In the left groin of a65-year-old patient, an oval-shaped lymph node is found inguinal, with a central proportion that is slightlyelevated in T2 weighted imaging indicating a normal fat hilus (**a**, *arrow*). The lymph node also shows a contrastuptake (**b**, T1w post contrast, *arrow*). Although the b1000 image of the DWI reveals an increased signal (**c**,*arrow*), there is no clear confirmation of a diffusion restriction in the ADC maps (**d**, *arrow*). Altgether, thelymph node was not considered suspicious for a metastatic involvement in MRI. In contrast to this, in the 68GaPSMA 11 PET/CT there is a high degree of certainty of a metastasis within the lymph node (**e** and **f**, *arrow*). **a**–**d**: MRI; **e**–**f**: 68Ga PSMA 11 PET/CT;**a**: T2w; **b**: contrast-enhanced T1w; **c**: b1000 DWI; **d**: ADC map; **e**: fusion of 68Ga PSMA 11 PET and low-dose CT; **f**: low-dose CT

CT, potentially reflecting the difficulty of imaging in the setting of altered, post-operative anatomy, the challenges of depicting small lymph node metastases [23], and the advantages of hybrid imaging with PET/CT combining both morphological and molecular data. Therefore, the inclusion of uncertain findings would, in our view, misleadingly favor MRI.

Our observation that 68Ga-PSMA-11 PET/CT detects more lesions characteristic for rPC compared to MRI is in agreement with several previous studies. For example, in a prospective study by Sawicki et al., superior detection rate for 68Ga-PSMA PET/CT in comparison to whole-body MRI was observed [24]. In a prospective study, Zacho et al. compared 68Ga-PSMA-11 PET/CT, 18F-sodium fluoride PET/CT, and diffusion-weighted MRI (DW600-MRI) for the detection of bone metastases in 68 patients with recurrent PCa, and observed that both PET methods performed better compared to DW600-MRI [25]. In a retrospective study, Rauscher et al. compared MRI with PET in 17 patients with recurrent PCa for the assessment of lymph node metastases, also noting the superiority of 68Ga-PSMA-11 PET/CT [26].

Most recently, Emmett et al. presented a prospective study including 91 patients with comparison of 18F-fluoro-methylcholine, multi-parametric MRI of the pelvis and 68Ga-PSMA-11 in men with biochemical failure after radical prostatectomy [27]. In this study, the authors reported a rate of pathologic 68Ga-PSMA-11 PET/CT in 42% of the patients, while pelvic MRI was pathologic in 28% of the patients, both findings being much lower than the detection rates revealed by our study. We interpret the lower median PSA in the study of Emmet et al. (0.42 ng/ml) compared to our patient cohort (median PSA of 1.9 ng/ml) as one potential explanation of this finding, noting the relationship between PSA value and detection rate in diagnostic modalities such as 68Ga-PSMA-11 PET/CT [7]. Notably, this study reports a larger relative difference in PSMA-PET/CT than MRI at this low PSA, potentially indicating the lower the PSA value the higher the margin of superiority for 68Ga-PSMA-11 PET/CT in comparison to MRI. Further studies with larger patient cohorts are required to confirm these results, which could inform a more tailored approach to the selection of imaging modalities for individual patients. We note that our patient cohort was too small for a statistically meaningful sub-analysis of the detection rates at different PSA values.

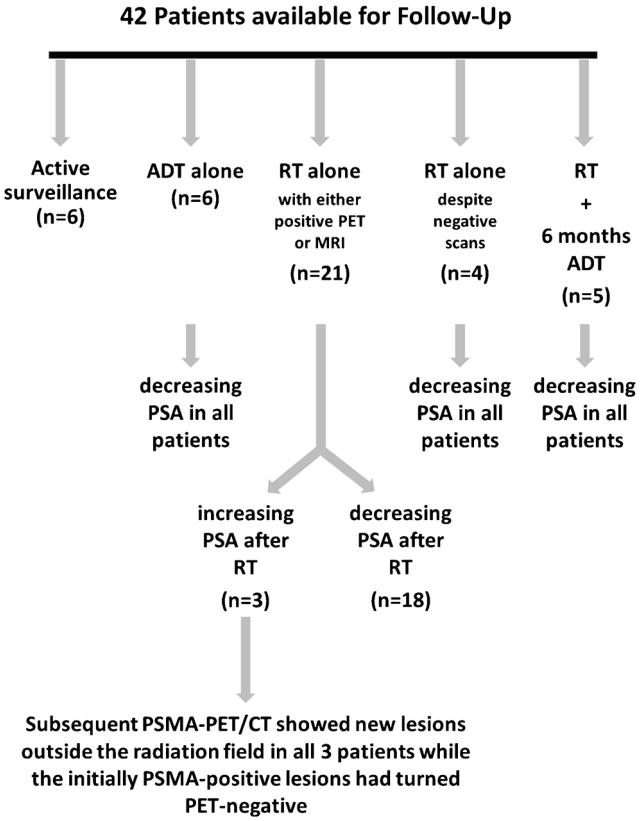

Fig. 6 Details of clinical follow-up. As shown by the figure, all PSMA-positive lesions and lesions suspicious of rPC in the MRI which were further treated with RT were most likely true-positive due to the subsequent decrease of PSA. None of the patients had surgical treatment or biopsies after the scans. *RT*: radiation therapy. *ADT*: androgen deprivation therapy

Emmett et al. included patients who had received all scans within a time window of 2 weeks. Although, for the purposes of inclusion, the nominal time window of our study was larger (2 months) we note that the mean time between examinations in our cohort was 9.6 days.

Our analysis of the follow-up data (available for 42 patients) showed that 32 patients went on to receive radiation therapy, either alone or in combination with other therapies. Of these patients, 20 received PET before MRI, whereas of the remaining patients who did not undergo RT, only four received PET before MRI. Although it is not possible to reconstruct the clinical decision-making in each individual case, we broadly interpret this small sample of results as a potential indication for the preference of MRI amongst our referring physicians for the purposes of planning radiation therapy. In this context, the superior resolution and soft-tissue contrast in MRI facilitates anatomical delineation of critical structures such as the bladder neck or rectum, which allows for improved treatment planning for RT [28].

Although this retrospective study did not include a gold standard, namely histopathological correlation of the imaging findings, in the 21 patients undergoing radiotherapy, 18 demonstrated a post-therapeutic fall in PSA, which we interpret as lending significant clinical weight to the diagnosis. Indeed, even if histological data were available, the lack of a standardized approach (e.g., patients with multiple surgically removed lymph node metastases would produce a bias) would mean that any such information would have to be interpreted with a great deal of caution. We are unable to reproduce the reasons for the second scan (either PET or MRI), and therefore cannot exclude selection bias in our cohort. Furthermore, given that all patients in our cohort presented with biochemical recurrence of PC, there were no true negative patients in our sample, precluding an analysis of the patient-based specificity, and negative as well as positive predictive values of the two modalities.

Drawing our various findings together, although our study confirms that 68Ga-PSMA-11 PET/CT can detect more lesions characteristic for rPC when compared to MRI, a complementary role for MRI is still to be found in the pre-treatment planning for RT. Ultimately, the combination of the advantages of both techniques represents a very promising imaging modality for patients with rPC [22, 29].

Conclusion

68Ga-PSMA-11 PET/CT detected more lesions characteristic for rPC compared to MRI. Our findings suggest that clinical algorithms should include 68Ga-PSMA-11 PET/CT for the initial staging of rPC, with the addition of MRI for treatment planning and for further clarification of unclear PET-findings.

Compliance with ethical standards

Ethical approval This evaluation was approved by the ethics committee of the University of Bern (KEK-Nr. 2018–00299). All patients published in this manuscript signed a written informed consent form for the purpose of anonymized evaluation and publication of their data.

Conflict of interest All authors declare that they have no conflict of interest.

References

1. Bray F, Ferlay J, Soerjomataram I, Siegel RL, Torre LA, Jemal A. Global cancer statistics 2018: GLOBOCAN estimates of incidence and mortality worldwide for 36 cancers in 185 countries. CA Cancer J Clin. 2018;68:394–424. https://doi.org/10.3322/caac.21492.
2. Wong MC, Goggins WB, Wang HH, Fung FD, Leung C, Wong SY, et al. Global incidence and mortality for prostate cancer: analysis of temporal patterns and trends in 36 countries. Eur Urol. 2016;70:862–74. https://doi.org/10.1016/j.eururo.2016.05.043.
3. Kessler B, Albertsen P. The natural history of prostate cancer. Urol Clin N Am. 2003;30:219–26.
4. Mottet N, Bellmunt J, Bolla M, Briers E, Cumberbatch MG, De Santis M, et al. EAU-ESTRO-SIOG Guidelines on Prostate Cancer. Part 1: screening, diagnosis, and local treatment with curative

intent. Eur Urol. 2017;71:618–29. https://doi.org/10.1016/j.eururo.2016.08.003.
5. Afshar-Oromieh A, Avtzi E, Giesel FL, Holland-Letz T, Linhart HG, Eder M, et al. The diagnostic value of PET/CT imaging with the (68)Ga-labelled PSMA ligand HBED-CC in the diagnosis of recurrent prostate cancer. Eur J Nucl Med Mol Imaging. 2015;42:197–209. https://doi.org/10.1007/s00259-014-2949-6.
6. Afshar-Oromieh A, Haberkorn U, Eder M, Eisenhut M, Zechmann CM. [68Ga]Gallium-labelled PSMA ligand as superior PET tracer for the diagnosis of prostate cancer: comparison with 18F-FECH. Eur J Nucl Med Mol Imaging. 2012;39:1085–6. https://doi.org/10.1007/s00259-012-2069-0.
7. Afshar-Oromieh A, Holland-Letz T, Giesel FL, Kratochwil C, Mier W, Haufe S, et al. Diagnostic performance of (68)Ga-PSMA-11 (HBED-CC) PET/CT in patients with recurrent prostate cancer: evaluation in 1007 patients. Eur J Nucl Med Mol Imaging. 2017;44:1258–68. https://doi.org/10.1007/s00259-017-3711-7.
8. Afshar-Oromieh A, Malcher A, Eder M, Eisenhut M, Linhart HG, Hadaschik BA, et al. PET imaging with a [68Ga]gallium-labelled PSMA ligand for the diagnosis of prostate cancer: biodistribution in humans and first evaluation of tumour lesions. Eur J Nucl Med Mol Imaging. 2013;40:486–95. https://doi.org/10.1007/s00259-012-2298-2.
9. Afshar-Oromieh A, Zechmann CM, Malcher A, Eder M, Eisenhut M, Linhart HG, et al. Comparison of PET imaging with a (68)Ga-labelled PSMA ligand and (18)F-choline-based PET/CT for the diagnosis of recurrent prostate cancer. Eur J Nucl Med Mol Imaging. 2014;41:11–20. https://doi.org/10.1007/s00259-013-2525-5.
10. Eiber M, Maurer T, Souvatzoglou M, Beer AJ, Ruffani A, Haller B, et al. Evaluation of hybrid 68Ga-PSMA ligand PET/CT in 248 patients with biochemical recurrence after radical prostatectomy. J Nucl Med. 2015;56:668–74. https://doi.org/10.2967/jnumed.115.154153.
11. Rauscher I, Duwel C, Haller B, Rischpler C, Heck MM, Gschwend JE, et al. Efficacy, predictive factors, and prediction nomograms for (68)Ga-labeled prostate-specific membrane antigen-ligand positron-emission tomography/computed tomography in early biochemical recurrent prostate cancer after radical prostatectomy. Eur Urol. 2018;73:656–61. https://doi.org/10.1016/j.eururo.2018.01.006.
12. Afshar-Oromieh A, Babich JW, Kratochwil C, Giesel FL, Eisenhut M, Kopka K, et al. The rise of PSMA ligands for diagnosis and therapy of prostate cancer. J Nucl Med. 2016;57:79S–89S. https://doi.org/10.2967/jnumed.115.170720.
13. Rahbar K, Afshar-Oromieh A, Jadvar H, Ahmadzadehfar H. PSMA theranostics: current status and future directions. Mol Imaging. 2018;17:1536012118776068. https://doi.org/10.1177/1536012118776068.
14. Eiber M, Fendler WP, Rowe SP, Calais J, Hofman MS, Maurer T, et al. Prostate-specific membrane antigen ligands for imaging and therapy. J Nucl Med. 2017;58:67S–76S. https://doi.org/10.2967/jnumed.116.186767.
15. Sahlmann CO, Meller B, Bouter C, Ritter CO, Strobel P, Lotz J, et al. Biphasic (6)(8)Ga-PSMA-HBED-CC-PET/CT in patients with recurrent and high-risk prostate carcinoma. Eur J Nucl Med Mol Imaging. 2016;43:898–905. https://doi.org/10.1007/s00259-015-3251-y.
16. Herlemann A, Wenter V, Kretschmer A, Thierfelder KM, Bartenstein P, Faber C, et al. (68)Ga-PSMA positron emission tomography/computed tomography provides accurate staging of lymph node regions prior to lymph node dissection in patients with prostate cancer. Eur Urol. 2016;70:553–7. https://doi.org/10.1016/j.eururo.2015.12.051.
17. Maurer T, Weirich G, Schottelius M, Weineisen M, Frisch B, Okur A, et al. Prostate-specific membrane antigen-radioguided surgery for metastatic lymph nodes in prostate cancer. Eur Urol. 2015;68:530–4. https://doi.org/10.1016/j.eururo.2015.04.034.
18. Pfister D, Porres D, Heidenreich A, Heidegger I, Knuechel R, Steib F, et al. Detection of recurrent prostate cancer lesions before salvage lymphadenectomy is more accurate with (68)Ga-PSMA-HBED-CC than with (18)F-Fluoroethylcholine PET/CT. Eur J Nucl Med Mol Imaging. 2016;43:1410–7. https://doi.org/10.1007/s00259-016-3366-9.
19. Hijazi S, Meller B, Leitsmann C, Strauss A, Meller J, Ritter CO, et al. Pelvic lymph node dissection for nodal oligometastatic prostate cancer detected by 68Ga-PSMA-positron emission tomography/computerized tomography. Prostate. 2015;75:1934–40. https://doi.org/10.1002/pros.23091.
20. Eder M, Neels O, Muller M, Bauder-Wust U, Remde Y, Schafer M, et al. Novel preclinical and radiopharmaceutical aspects of [68Ga]Ga-PSMA-HBED-CC: a new pet tracer for imaging of prostate cancer. Pharmaceuticals. 2014;7:779–96. https://doi.org/10.3390/ph7070779.
21. Bashir U, Tree A, Mayer E, Levine D, Parker C, Dearnaley D, et al. Impact of Ga-68-PSMA PET/CT on management in prostate cancer patients with very early biochemical recurrence after radical prostatectomy. Eur J Nucl Med Mol Imaging. 2019;46(4):901–7. https://doi.org/10.1007/s00259-018-4249-z.
22. Afshar-Oromieh A, Haberkorn U, Schlemmer HP, Fenchel M, Eder M, Eisenhut M, et al. Comparison of PET/CT and PET/MRI hybrid systems using a 68Ga-labelled PSMA ligand for the diagnosis of recurrent prostate cancer: initial experience. Eur J Nucl Med Mol Imaging. 2014;41:887–97. https://doi.org/10.1007/s00259-013-2660-z.
23. Maurer MH, Harma KH, Thoeny H. Diffusion-weighted genitourinary imaging. Urol Clin North Am. 2018;45:407–25. https://doi.org/10.1016/j.ucl.2018.03.003.
24. Sawicki LM, Kirchner J, Buddensieck C, Antke C, Ullrich T, Schimmoller L, et al. Prospective comparison of whole-body MRI and (68)Ga-PSMA PET/CT for the detection of biochemical recurrence of prostate cancer after radical prostatectomy. Eur J Nucl Med Mol Imaging. 2019;46(7):1542–50. https://doi.org/10.1007/s00259-019-04308-5.
25. Zacho HD, Nielsen JB, Afshar-Oromieh A, Haberkorn U, deSouza N, De Paepe K, et al. Prospective comparison of (68)Ga-PSMA PET/CT, (18)F-sodium fluoride PET/CT and diffusion weighted-MRI at for the detection of bone metastases in biochemically recurrent prostate cancer. Eur J Nucl Med Mol Imaging. 2018;45:1884–97. https://doi.org/10.1007/s00259-018-4058-4.
26. Rauscher I, Maurer T, Beer AJ, Graner FP, Haller B, Weirich G, et al. Value of 68Ga-PSMA HBED-CC PET for the assessment of lymph node metastases in prostate cancer patients with biochemical recurrence: comparison with histopathology after salvage lymphadenectomy. J Nucl Med. 2016;57:1713–9. https://doi.org/10.2967/jnumed.116.173492.
27. Emmett L, Metser U, Bauman G, Hicks RJ, Weickhardt A, Davis ID, et al. A prospective, multi-site, international comparison of F-18 fluoro-methyl-choline, multi-parametric magnetic resonance and Ga-68 HBED-CC (PSMA-11) in men with high-risk features and biochemical failure after radical prostatectomy: clinical performance and patient outcomes. J Nucl Med. 2018;60(6):794–800. https://doi.org/10.2967/jnumed.118.220103.
28. Moghanaki D, Turkbey B, Vapiwala N, Ehdaie B, Frank SJ, McLaughlin PW, et al. Advances in prostate cancer magnetic resonance imaging and positron emission tomography-computed tomography for staging and radiotherapy treatment planning. Semin Radiat Oncol. 2017;27:21–33. https://doi.org/10.1016/j.semradonc.2016.08.008.
29. Hope TA, Afshar-Oromieh A, Eiber M, Emmett L, Fendler WP, Lawhn-Heath C, et al. Imaging prostate cancer with prostate-specific membrane antigen PET/CT and PET/MRI: current and future applications. AJR Am J Roentgenol. 2018;211:286–94. https://doi.org/10.2214/AJR.18.19957.